High-speed spindle dynamic error separation technique

V. Joseph Pannackal, S. Fletcher, A.P. Longstaff, N. Mian
University of Huddersfield, United Kingdom

Abstract

The accuracy of a subtractive machining process is affected by the error motions of the machine tool spindle. Excessive error or concern over the spindle condition can cause unscheduled downtime, scrap or rework, unexpected production delays, and customer disappointment. There are various techniques and measurement systems available for spindle error motion measurement. They typically include the use of several displacement sensors and a test bar. Different methods are available for the separation of spindle error motion from the roundness error of the test bar. The three main types of spindle error separation techniques are reversal, multi-probe, and multi-step approaches. The Donaldson reversal method is a common technique used for spindle error separation. In this method the artefact (test bar) and displacement sensor needed to be physically rotated to obtain each measurement.

In this research, a new implementation of the Donaldson reversal technique with multiple probes is developed so that the manual rotation of the measurement setup is not required. The artefact and spindle error motions are simulated in a computer-generated model. Various thermo-mechanical errors were introduced to evaluate the performance of the error separation algorithm for high-speed applications. The simulation result indicates that the effect of test bar roundness error along with external random errors has been separated and most of the system effects have been reduced. The outcome of this research can be used in an industrial spindle error measurement system.

1 Introduction

The accuracy of a machine tool spindle is a fundamental requirement of any high-precision machine. A machine tool consists of one or more linear or rotary axis. The spindle rotates the tool or workpiece around an axis of rotation. Many factors

can cause errors in spindle motion. In ultra-precision manufacturing, it is always desirable to reduce the errors to the least possible value.

There are different sources of spindle error motions [1-3], which include the imperfection in the bearing geometry, structural error motions and thermal effects. When measuring the error motion, external error sources such as machine and floor vibration, artefact (test bar) form error, ambient temperature, and other noise sources influence the measurement system which necessitate the use of an error separation method [4]. There are various techniques used in metrology for spindle error separation. According to *Chen et al.* [5], there are mainly three different methods for error separation of spindle error measurement which are reversal, multi-probe and multistep.

Multiple measurements are made for each spindle error component in the multistep method. Typically, the artefact is rotated in equal steps with respect to the probe for measuring the error components [6]. According to *Linxiang* [7], the multistep technique is suitable for high precision roundness error of a machine tool. Although the measurement can be recorded in the nanometric range, the error separation accuracy is questionable in this method due to the cumulative uncertainty in multiple measurement steps.

The multi-probe method performs the error measurement simultaneously with three or more probes [6]. *Whitehouse* [8] explained that the multiprobe system could eliminate any desired order of variable error, but it is susceptible to harmonic suppression. Even though this method produced adequate results, the multi-probe method requires proper orientation of the sensors. Any deviation from the orientation can cause measurement errors.

The reversal method is regarded as a commonly used ‘complete’ error separation technique. *Evans et al.* [9] discuss many strategies, such as Donaldson reversal, Estler's reversal, level reversal, and straightedge reversal. This method requires two measurements to compute a single component of spindle error [6]. Both the displacement sensor and the artefact are turned in the Donaldson reversal technique for accurately separating the spindle error motion from part error [10, 11].

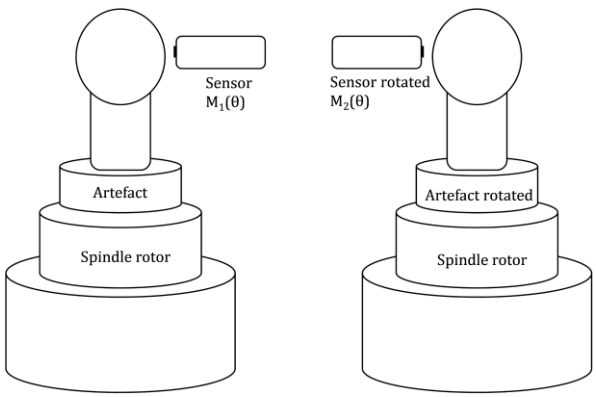

Figure 1: Donaldson reversal (modified from [11])

In Donaldson reversal, two radial error measurements are taken at $M_1(\theta)$ and $M_2(\theta)$ as shown in figure 1. The artefact and sensor assembly are rotated by 180° to perform these two measurements. The 'θ' represents the degree of rotation. The artefact's form error and spindle error motion (radial) are represented by $A(\theta)$ and $S(\theta)$ respectively. Then according to Donaldson reversal technique [11] :

$$M_1(\theta)= A(\theta)+S(\theta) \quad (1)$$
$$M_2(\theta)= A(\theta)-S(\theta) \quad (2)$$

The spindle error motion and artefact's form error can be easily obtained and is represented in equations 3and 4.

$$S(\theta)= (M_1(\theta)- M_2(\theta))/2 \quad (3)$$
$$A(\theta)= (M_1(\theta)+ M_2(\theta))/2 \quad (4)$$

While this method accurately separates spindle error from part error, rotating both probes and the artefact by 180° is not always feasible [12]. This research work aims to create a measurement system, utilising two sensors to perform a reversal which can eliminate the manual reversal problem associated with this technique. Since this is an extension of Donaldson reversal technique and the results are obtained using software, the new approach is referred as Digital Donaldson Reversal (DDR) throughout the report.

2 Spindle error separation model

In this research, the simulated evaluation of the proposed DDR is performed. The LabVIEW software [13] is used to generate the various error signals including the spindle, test bar, external vibration errors and evaluate the error separation in accordance with ISO 230-7:2015 [1]. For the DDR approach, two sensors are kept a nominal 180° apart. Any position error of the sensor can be compensated within the software or at the data processing stage. The position of the sensor and artefact (test bar) is shown in figure 2. The total error motion of the spindle and the contribution of external error sources are generated in this simulation.

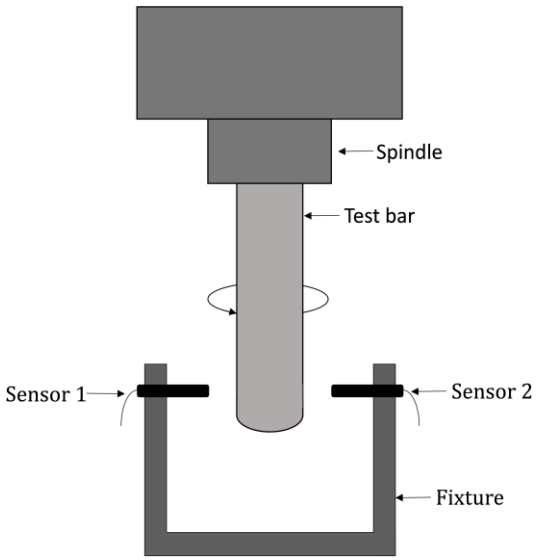

Figure 2: Test setup for radial error motion

In this research, only the radial error motion of a single axis is considered. The knowledge is transferable to measure the radial error motion of the other axes and tilt of the machine tool spindle. This method can be applied with any type of non-contact displacement sensor with submicron resolution and sufficient bandwidth. It can be capacitive, inductive or optical sensors, and the test mandrel selection will be based on the sensor used. The total error motion of the spindle consists of both synchronous and asynchronous radial error motions. One of the main contributing factors towards the structural spindle error motion is the 'noisy rolling element bearings' [1]. For the simulation, the rolling element defects such as inner and outer ball pass frequencies, fundamental train frequency, and the ball spin frequency is calculated. General equations were derived to obtain the values of bearing fault frequencies and is shown in Table 1 [14, 15].

Table 1: Bearing fault frequency (Hz)

Ball Pass Frequency Inner (BPFI)	12.773×(RPM/60)
Ball Pass Frequency Outer (BPFO)	11.227×(RPM/60)
Ball Spin Frequency (BSP)	14.938×(RPM/60)
Fundamental Train Frequency (FTF)	0.4678×(RPM/60)

Different types of external errors that affect the measurement are considered in this simulation. The parameters of these error noises are obtained from the real time data of the spindle error measurement system. Simulation is then carried out with these parameters in the LabVIEW software. Since two sensors are involved in the DDR technique, two sets of combined error signals are obtained.

3 Implementation of Digital Donaldson Reversal (DDR)

As mentioned in section 2, the original spindle error motion consists of different bearing fault frequencies. Figure 3.a shows the polar representation of the total error motion of the machine spindle deriving from the four bearing fault frequencies given in Table 2. The speed of the machine spindle is considered as 10000 RPM. Substituting this in the equations at table 1, we get the values of bearing fault frequencies as shown in Table 2.

Table 2: Bearing fault frequency.

Ball Pass Frequency Inner (BPFI)	2128.83 Hz
Ball Pass Frequency Outer (BPFO)	1870.5 Hz
Ball Spin Frequency (BSP)	2489.67 Hz
Fundamental Train Frequency (FTF)	77.9667 Hz

Table 3: Parameters of the simulation.

S No	**Parameter**	**Specification value**
1	Spindle speed (RPM)	10,000 RPM
2	Spindle speed (Hz)	166.67 Hz
3	TIR amplitude	10 µm
4	BPFI value	0.5 µm
5	BPFO	0.45 µm
6	BSP	0.35 µm
7	FTF	0.15 µm
8	Vibration (Common to both)	0.91 µm
9	Vibration frequency (Common to both, E_1)	900 Hz
10	Noise (Common to both)	0.45 µm
11	Noise frequency (Common to both, E_2)	1450 Hz
12	Noise at Sensor 1	0.62 µm
13	S1 Noise Frequency (E_3')	550 Hz
14	Noise at Sensor 2	0.55 µm
15	S2 Noise Frequency (E_4')	450 Hz

Traditionally, separating the spindle error motion and the artifact's (test bar) form error utilises the data obtained from the displacement sensor. In this simulation, the artefact's form error is generated as random error signal. However, several other sources of external errors like the noise from the vibration of the machine tool and the local environment which may be a busy factory shop floor. Furthermore, the effects of ambient temperature, fluctuations in the power supply, electro-magnetic interferences, light interference (for optical sensors), etc. affect both sensors simultaneously. DDR simulation combines all these errors and sums it up to two main errors, one is dedicated to the vibration (E_1) while the other is considered as the sum of all other errors including the artefact's form error (E_2).

These two types of error signals are generated to create the effect of contemporaneous error at both the sensors (E_1 & E_2).

Although the sensors are linear and calibrated, there are some non-uniform conditions that can cause measurement error. This error varies with respect to the sensor. Since this type of error is sensor-dependent, two different noise signals are generated that corresponds to the two sensors (E_3' & E_4'). So, altogether there are three types of error signals considered in each sensor. For sensor 1 and sensor 2 two error signals remains the same (E_1 & E_2) while the third one differs (E_3' & E_4'), that corresponds to the sensor-dependent error. The parameters used in the simulation are shown in Table 3.

4 Simulation results

The DDR simulation was performed, and the error separation was executed. The results obtained are analysed in the following section. Figures 3 and 4 depict the polar representation of the error separation. The green and black circles represent the range of maximum and minimum values respectively. The average of the error data is indicated by the red circle. It is assumed that a trigger signal can be used to ensure accurate extraction of the data sets for each revolution of the artefact.

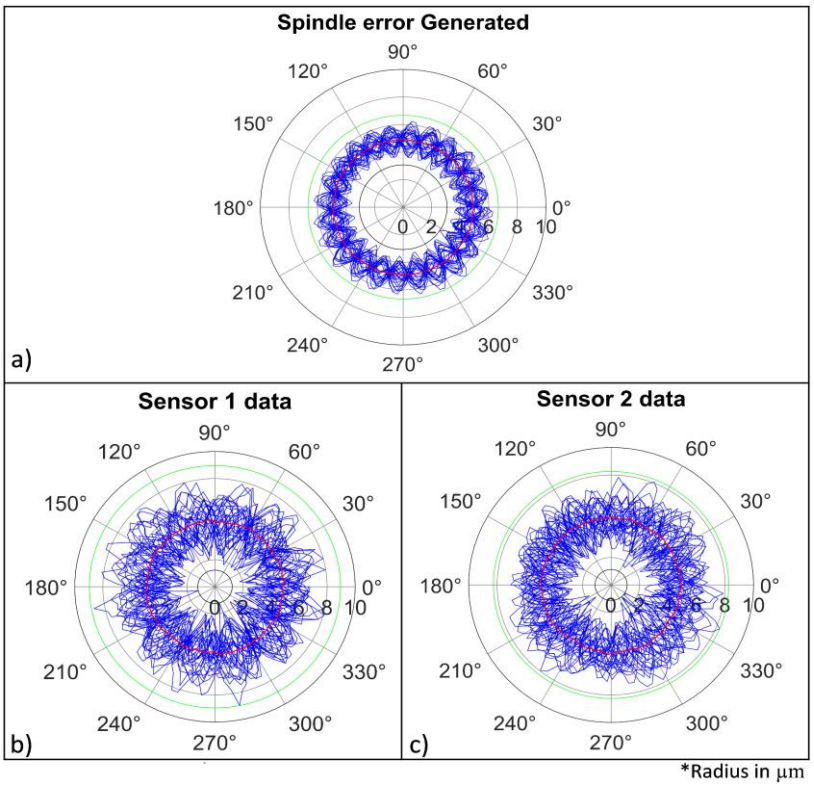

Figure 3: Polar Plot of (a) Generated spindle data, (b) Sensor 1 and (c) Sensor 2

The simulated spindle error motion that consists of bearing faults and radial error motion is depicted in figure (3.a). The measured output (simulated) corresponding to both sensors are shown in figure (3.b) and (3.c). After analysing the data from sensor 1 and sensor 2, the effect of the external error noises (E_1, E_2, E_3' & E_4') are clearly visible. The polar representation has a circular shape because this simulation does not consider the variable stiffness within the spindle axis or the supporting machine structure.

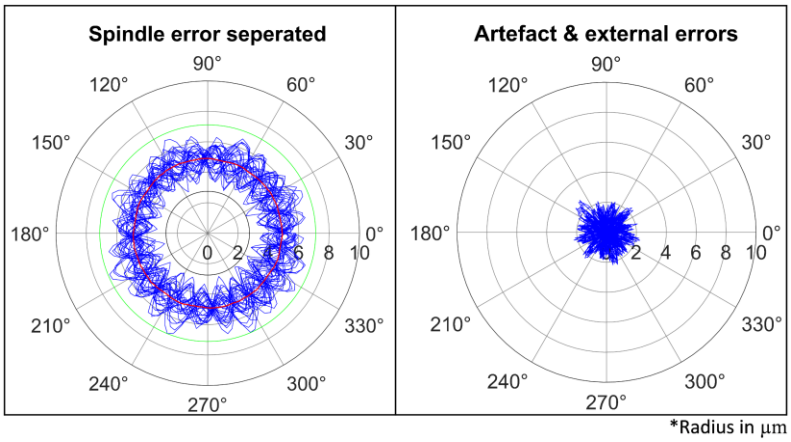

Figure 4: Polar Plot of (a) Separated spindle error motion and (d) Artefact & external errors

The Digital Donaldson Reversal technique has separated the external error sources from the original spindle error motion, shown in figure 4. The separated artefact error signal consists of most of the supplied error signal. The frequency analysis will provide more insights about the error separation.

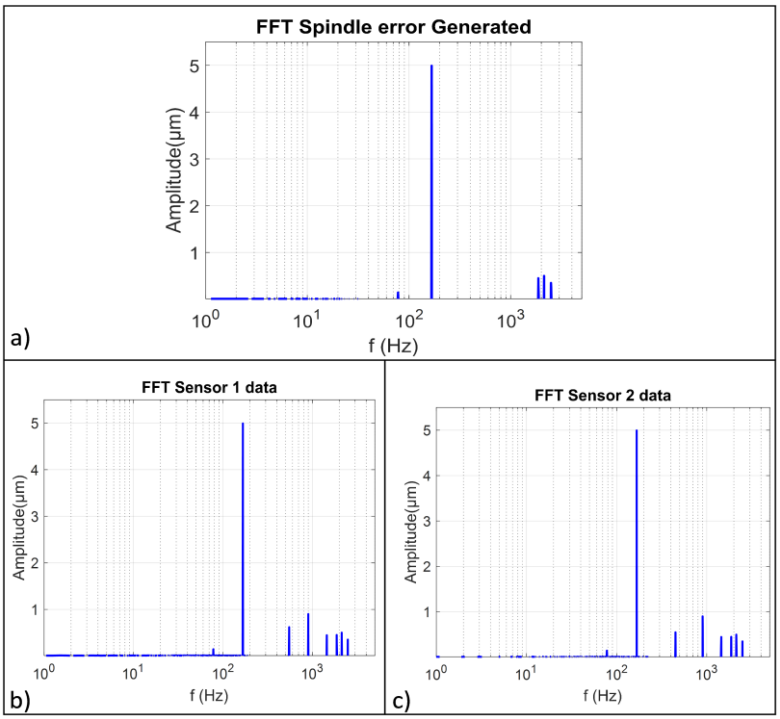

Figure 5: FFT of (a) Generated spindle data, (b) Sensor 1 and (c) Sensor 2

The FFT of generated spindle error signal (figure (5.a)) shows the radial motion of the spindle at 166.67Hz (10000 RPM) along with bearing fault frequencies at 77.9667 Hz (FTF), 1870.5 Hz (BPFO), 2128.83 Hz (BPFI), and 2489.67 Hz (BSF). In addition to the spindle error motion frequencies, the sensors indicate the supplied external error frequencies (figure (5.b) & (5.c)). Both sensors have contemporaneous errors with 900 Hz (E_1) and 1450 Hz (E_2). Sensor 1 has a separate noise of 550 Hz (E_3'), and sensor 2 has the same at 450 Hz (E_4').

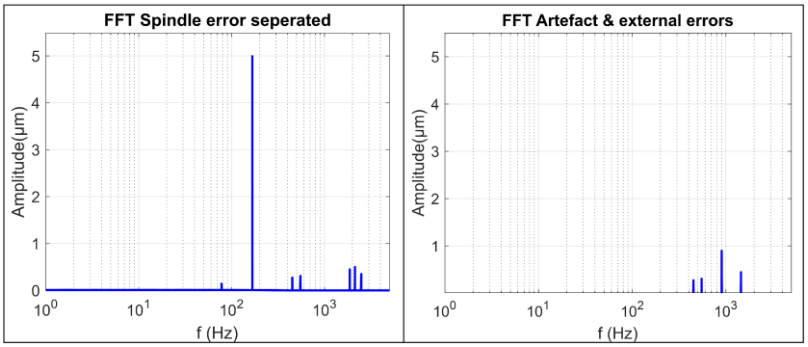

Figure 6: FFT of (a) Separated spindle error motion and (b) Artefact & external errors

The separated artefact error signal (figure (6.b)) consists of error frequencies at 450 Hz, 550 Hz, 900 Hz and 1450 Hz. The separated spindle error (figure (6.a)) signal indicates spindle error frequencies of 77.9667 Hz, 166.67 Hz, 1870.5 Hz, 2128.83 Hz and 2489.67 Hz, and the external error frequencies of 450 Hz and 550 Hz. The results of the DDR technique separate the contemporaneous external errors completely, while individual error noise is partially separated.

From practical test data, the effect of the individual error noise can be assumed to be minimal. The amplitude observed for this error was in the submicron (less than 0.1µm). An error compensation system can reduce the effect of this error. This will be the future work, along with the selection of a suitable displacement sensor.

Nevertheless, the DDR technique was able to separate all forms of error noises, including the prominent vibration and artefact form errors. Multiple sensor pair combination may be employed to measure the radial, axial and tilt motion of a machine tool spindle. This technique could be applied with low-cost displacement sensors so that it may be able to replace costly conventional sensor systems.

5 Conclusion

Spindle measurement may employ the Donaldson reversal method which is performed by manual reversal of the test mandrel and displacement sensor. In this paper, a new system is proposed to eliminate this manual reversal using a dual opposing sensor approach. The radial error motion of the machine spindle was generated and supplied with various thermo-mechanical errors. The simulation results showed that prominent random external effects besides the test bar error were separated completely while most of the system effects has been reduced to 50%. The future scope of the project is to create error compensation system to decrease the effect of the systematic errors.

Acknowledgement

The authors gratefully acknowledge the UK’s Engineering and Physical Sciences Research Council (EPSRC) funding of the Future Metrology Hub (Grant Ref: EP/P006930/1) and UKRI-funded Advanced Machinery and Productivity Initiative (84646).

References

[1] "BS ISO 230-7:2015: Test code for machine tools: Geometric accuracy of axes of rotation," ed: British Standards Institute, 2017.

[2] "BS ISO 230-1:2012: Test code for machine tools: Geometric accuracy of machines operating under no-load or quasi-static conditions," ed: British Standards Institute, 2012.

[3] J. Chrzanowski, T. Sałaciński, and P. Skiba, "Spindle error movements and their measurement," *Applied sciences*, vol. 11, no. 10, p. 4571, 2021, doi: 10.3390/app11104571.

[4] Y. Chen, X. Zhao, W. Gao, G. Hu, S. Zhang, and Y. Tian, "A novel measuring module for spindle rotational accuracy based on virtual instrument," *Advances in mechanical engineering*, vol. 9, no. 11, pp. 1-11, 2017, doi: 10.1177/1687814017730754.

[5] Y. Chen, X. Zhao, W. Gao, G. Hu, S. Zhang, and D. Zhang, "A novel multi-probe method for separating spindle radial error from artifact roundness error," *International journal of advanced manufacturing technology*, vol. 93, no. 1-4, pp. 623-634, 2017, doi: 10.1007/s00170-017-0533-5.

[6] E. R. Marsh, "4.4 Multiposition Error Separation," in *Precision Spindle Metrology (2nd Edition)*: DEStech Publications, 2010, p. 82.

[7] C. Linxiang, "The measuring accuracy of the multistep method in the error separation technique," *Journal of physics. E, Scientific instruments*, vol. 22, no. 11, pp. 903-906, 1989, doi: 10.1088/0022-3735/22/11/002.

[8] D. J. Whitehouse, "Some theoretical aspects of error separation techniques in surface metrology," *Journal of physics. E, Scientific instruments*, vol. 9, no. 7, pp. 531-536, 1976, doi: 10.1088/0022-3735/9/7/007.

[9] C. J. Evans, R. J. Hocken, and W. T. Estler, "Self-Calibration: Reversal, Redundancy, Error Separation, and 'Absolute Testing'," *CIRP annals*, vol. 45, no. 2, pp. 617-634, 1996, doi: 10.1016/S0007-8506(07)60515-0.

[10] J. G. Salsbury, "Implementation of the Estler face motion reversal technique," *Precision engineering*, vol. 27, no. 2, pp. 189-194, 2003, doi: 10.1016/S0141-6359(02)00190-3.

[11] S. Cappa, D. Reynaerts, and F. Al-Bender, "A sub-nanometre spindle error motion separation technique," (in English), *Precision engineering*, vol. 38, no. 3, pp. 458-471, 2014, doi: 10.1016/j.precisioneng.2013.12.011.

[12] B. Muralikrishnan and J. Raja, *Computational surface and roundness metrology*, 1. Aufl. ed. (no. Book, Whole). London: Springer, 2009.

[13] *LabVIEW 2020*. (2020). [Online]. Available: https://www.ni.com/en-gb/shop/labview.html

[14] A. Hemati, "A Case Study: Fluting Failure Analysis by Using Vibrations Analysis," *Journal of failure analysis and prevention*, vol. 19, no. 4, pp. 917-921, 2019, doi: 10.1007/s11668-019-00715-w.

[15] L. Renaudin, F. Bonnardot, O. Musy, J. B. Doray, and D. Rémond, "Natural roller bearing fault detection by angular measurement of true instantaneous angular speed," *Mechanical systems and signal processing*, vol. 24, no. 7, pp. 1998-2011, 2010, doi: 10.1016/j.ymssp.2010.05.005.